Journal of Engineering and Applied Sciences 2 (4): 798-807, 2007

Multiple Model Approach Modelling: Application to a Turbojet Engine

[1]Abdelkader Akhenak, [2]Mohammed Chadli, [1]José Ragot, [1]Didier Maquin
[1]Centre de Recherche en Automatique de Nancy, CNRS UMR 7039,
Institut National Polytechnique de Lorraine,
Avenue de la forêt de Haye, 54516 Vandoeuvre-les-Nancy Cedex, France
[2]Centre de Robotique, d'Electrotechnique et d'Automatique,
Université de Picardie-Jules Verne 7, Rue du Moulin Neuf-80000 Amiens, France

Abstract: In this study, we show the interest of multiple model modelling approach to apprehend nonlinear behaviors of physical systems. From experimental data, we develop a model of simple structure which can be exploited in many Fields such as control, diagnosis or for the design of observers. An application on a turbojet plane is presented.

Key words: Multiple model approach, nonlinear system, turbojet engine

INTRODUCTION

The use of mathematical models in engineering sciences has grown with electronic and power computer development, especially in aeronautic and more precisely in aircraft engine's manufacture. These models are used in order to calculate dimension, to design numeric control systems, or to design diagnosis algorithms. To underline our industrial interest, we work with a 2-shaft engine support.

Turbojet engine's principle is the ejection of gas mass faster than the aircraft speed. The thrust depends of: the difference between inlet and exit gas speed, the gas mass fow in the engine, the difference between inlet and exit static pressure area. Therefore the engine is the assembly of the following components (Fig. 1):

- Fan (1),
- Low Pressure compressor (LP) (2),
- High Pressure compressor (HP) (3),
- Burner (4),
- Turbine HP (5),
- Turbine BP (6),
- Nozzle (7).

The fan controls the inlet air fow. The two stages of the compressor allow an easier pressure burner adaptation in whole fight conditions. Burner warms up the mixed gas air and fuel. The gas speed is then increased and a part of the power is used by turbines in order to drive compressors in rotation. The gas is also accelerated into the exhaust nozzle after the turbines.

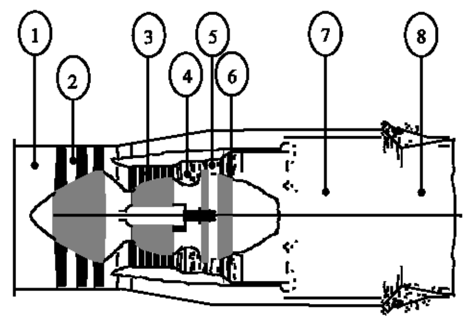

Fig. 1: Section of turbojet engine

A turbojet engine includes a lot of equipment in order to know its states and to control it. The knowledge of the states (LP and HP speed, pressure and temperature at different stages) is done by means of sensors and actuators allow to control it to reach the expected thrust. Principal actuators are: fuel metering valve, variable stator valve (which modify the geometry of some compressor stages in order to avoid the surge phenomena) and bleed valve (which takes air to avoid the surge phenomena).

From the middle of the sixties to the beginning of the seventies, we could note an interest in mathematical modelization of aircraft engines to design control systems. In 1971, Mueller, designs a linear model of a 2-shaft aircraft engine which allows to Find overall conditions of

Corresponding Author: Abdelkader Akhenak, Centre de Recherche en Automatique de Nancy, CNRS UMR 7039, Institut National Polytechnique de Lorraine, Avenue de la forêt de Haye, 54516 Vandoeuvre-les-Nancy Cedex, France

stability, observability and controllability. At the end of the seventies and in the beginning of the eighties, appear the First works in control (Trevino and Olcmen, 2003; Harefors, 1997) and diagnosis (Savy, 2003; Wu and Campion, 2004) using mathematical models in order to estimate directly in real time engine's outputs like in (Wells and Dsilva, 1977) or to simulate the engine's outputs like in (Dsilva, 1982). In the middle of the 80s, numerical control systems appeared and then the use of models became necessary.

Different kinds of engine's model exist: static thermodynamical models, dynamic thermodynamical models, correlated engine sensor measurement models and linear models in different operating points. Static thermodynamical models are a thermodynamical and a thermical phenomena representation of the different stages of the engine. Each stage is linked to the next by static continuous equations. Dynamic thermodynamical models are dynamic representation of thermodynamical and thermical phenomena (like thermical exchanges) between the following stages: HP compresser, burner and HP turbine. Correlated measurement models are often polynomial representations of a series of measurements. Linear models are linearization of the engine's equations at different points.

Thermodynamical models are usually used to calculate the dimensions of the engine's components in order to satisfy customers expectations and also to design and simulate control systems. The two others are usually onboard models used for diagnosis algorithms like in (Mueller, 1971).

Aircraft engine is a strongly non linear system and its continuous representation is difficult. For that, there are a lot of table and switch in the above models description. These tools are not continuous and then could be source of troubles either in control algorithm robustness or in decision logic in diagnosis. Moreover many efficient control and diagnosis methods have been developed in continuous time. The present study aims to establish, on the basis of a nonlinear model which parameters are defined by a lookup table, a global continuous model. Our research basis is a 2-shaft aircraft engine illustrated by Fig. 1, the units of the variables are not given for reasons of conFidentiality. The model structure is represented by two dynamical equations:

$$\begin{cases} \dot{x}_1 = K_1\ (x_1)\ (x_2 - y_2R\,(x_1)) + K_2\,(x_1)\ (u - uR\,(x_1)) \\ \dot{x}_2 = K_3\ (x_1)\ (x_2 - y_2R\,(x_1)) + K_4\,(x_1)\ (u - uR\,(x_1)) \end{cases} \quad (1)$$

and 4 output equations:

$$\begin{cases} y_1 = x_1 \\ y_2 = x_2 \\ y_3 = K_5(x_1)(x_2 - y_2R(x_1)) + K_6(x_1)(u - uR(x_1)) + y_3R(x_1) \\ y_4 = K_7(x_1)(x_2 - y_2R(x_1)) + K_8(x_1)(u - uR(x_1)) + y_4R(x_1) \end{cases} \quad (2)$$

In these equations, x_1 is the LP compressor speed, x_2 is the HP compressor speed, y_3 is the static pressure at the output of HP compressor, y_4 is the temperature in the burner and u is the fuel fow.

The parameter functions deFining the gains $K_i(x_1)$ and the offsets $y_2R(x_1)$, $y_3R(x_1)$, $y_4R(x_1)$ and $uR(x_1)$ are given for eight different operating points. Their values are collected in Table 1. In the sequel, the parameter functions $y_2R(x_1)$, $y_3R(x_1)$, $y_4R(x_1)$ and $uR(x_1)$ will be also denoted $K_9(x_1)$, $K_{10}(x_1)$, $K_{11}(x_1)$ and $K_{12}(x_1)$, respectively in order to be able to designate all the functions globally.

The various parameter functions they vary according to the state variable x_1. The numerical values of these gains are given by a cartography for 8 operating points, as one can see it on the Table 1. Then discontinuities of this look-up model are not easily exploitable either in the control or diagnosis Fields. Moreover, the methods developed in these two Fields are based preferably on continuous analytical models between the outputs and the state variables. Then, our objective is to obtain a valid total model on all the operation range. For that, it is preferable to represent this look-up model by an analytical

Table 1: Values of the parameter functions

x_1	33.58	49.30	59.60	64.46	75.02	79.89	89.19	93.48
K_1	0.8674	1.5000	2.2186	2.2989	1.8728	1.4068	1.2300	1.1320
K_2	0.04799	0.06927	0.07049	0.07255	0.07065	0.06575	0.06792	0.06931
K_3	-0.3266	-0.7633	-1.2828	-1.400	-1.1087	-0.9261	-1.1446	-1.2441
K_4	0.04884	0.04691	0.04237	0.03972	0.03521	0.03215	0.02889	0.02862
K_5	0.0615	0.1001	0.1416	0.1445	0.0998	0.07525	0.06125	0.05812
K_6	0.00253	0.00323	0.00316	0.00303	0.00291	0.00310	0.00305	0.00306
K_7	-9.23	-8.55	-9.83	-9.54	-5.625	-3.506	-1.656	-2.162
K_8	1.9926	1.1441	0.8702	0.7406	0.5477	0.4710	0.3578	0.3177
y_{2R}	56.94	69.09	74.25	76.80	82.50	86.93	93.11	95.03
y_{3R}	2.667	4.225	5.543	6.452	8.642	10.01	12.76	14.06
y_{4R}	630.0	649.3	680.5	712.5	776.5	824.2	899.5	930.2
u_R	155.1	259.0	364.3	451.6	675.9	840.4	1178.3	1346.9

model. The multiple model approach can apprehend nonlinear behaviors, while keeping the simplicity of the linear models. The proposed modelling approach is carried-out in two step:

First step: The parameter functions $K_i(x_1)$; i = 1, ..., 12, are modelled using a multiple model approach, based on the look-up table described in Table 1. Next, using these analytical nonlinear models, the global nonlinear model of the aircraft engine is established.

Second step: This global nonlinear analytical model is then linearized around some operating points in order to establish a multiple model of the behavior of the engine.

MULTIPLE MODEL APPROACH

The multiple model representation is an approach for modelling nonlinear dynamical systems (Johansen and Foss, 1993; Murray, 1997). The underlying idea is to apprehend the global behavior of a system by a set of local models (linear or affine), each local model characterizing the system's behavior in a particular zone of operation. The local models are then aggregated by the mean of an interpolation mechanism. The motivation of this approach comes from the fact that it is often difficult to design a model which takes into account all the complexity of the studied system.

Like any modelling problem, the identification of a multiple model leads to the search of the model structure and the estimation of its parameters. In the following section, one will be interested in the parametric optimization which consists in estimating the parameters of the activation functions and those of the local models. The considered multiple model is defined as follows:

$$\begin{cases} \dot{x}(t) = \sum_{i=1}^{M} \mu_i(\xi(t))(A_i x(t) + B_i u(t) + D_i) \\ y(t) = \sum_{i=1}^{M} \mu i(\xi(t))(C_i x(t) + L_i u(t) + S_i) \end{cases} \quad (3)$$

where $x(t) \in \mathbb{R}^n$ is the state vector, $u(t) \in \mathbb{R}^m$ is the input vector and $y(t) \in \mathbb{R}^p$ is the output vector. For the i th local model $Ai \in \mathbb{R}^{n\times n}$ is the state matrix, $Bi \in \mathbb{R}^{n\times m}$ and $Li \in \mathbb{R}^{n\times p}$ are the input matrices, $Ci \in \mathbb{R}^{p\times n}$ is the output matrix and $(Di; Si) \in \mathbb{R}^n \times \mathbb{R}^n$ are constant matrices.

The activation functions $\mu_i(\xi(t))$, i = {1, ..., M} have the following properties:

$$\begin{cases} \sum_{i=1}^{M} \mu_i(\xi(t) = 1 \\ 0 \le \mu_i(\xi(t)) \le 1 \ \forall_i \in \{1, ..., M\} \end{cases} \quad (4)$$

where $\xi(t)$ represents the decision vector depending on the input and/or the measurable state variables. The number of local models (M) depends on the desired modelling precision, the complexity of the nonlinear system and the choice of the structure of the activation functions.

A multiple model can be obtained by identification (Gasso *et al*., 2000), by linearization of known nonlinear model around various operating points (in this case each local model is an affine LTI system due to the presence of the constant of linearization) (Johansen and Foss, 1993; Murray, 1997) or by convex polytopic transformation (Tanake *et al*., 1996; Wang *et al*., 1996).

Representation of the parameter functions by multiple models: The First step of the proposed modelling approach consist to approximate the parameter functions $K_i(x_1)$, i = {1, ..., 12} using a multiple model approach on the basis of the given look-up Table 1. The analytical formulation of each gain is given by the following equation:

$$\hat{K}_i(x_1) = \sum_{j=1}^{M} \mu_{ij}(x_1)(\alpha_{ij} x_1 + \beta_{ij}), \ i = \{1, ..., 12\} \quad (5)$$

Where $\hat{K}_i(x_1)$ represents the approximation of the parameter function $K_i(x_1)$, M is the number of local models, α_{ij} and β_{ij} are parameters to be identified by a parametric optimization method. $\mu ij(x_1)$ represents the activation function of the j th local model which indicates the degree of activation of this model in its operating zone, the index i is related to the i th gain. According to the number M of the local models, the activation functions take different form. For M = 2, we have:

$$\mu_{i1}(x_1) = \exp\left(\frac{-(x_1 - b_{i1})\ 2}{2a_{i1}^2}\right) \text{and } \mu_{i2}(x_1) = 1 - \mu_{i1}(x_1)$$

If M > 2, the activation functions are as follows:

$$w_{i1}(x_1) = \frac{1}{1 + \exp\left(\frac{-a_{i1}}{x_1 - b_{i1}}\right)}, \ w_{ij}(x_1) = \exp\left(\frac{-(x_1 - b_{ij})^2}{2a_{ij}^2}\right)$$

with $1 < j < M$

$$w_{iM}(x_1) = \frac{1}{1 + \exp\left(\frac{-a_{iM}}{x_1 - b_{iM}}\right)}, \ \mu_{ij}(x_1) = \frac{w_{ij}(x_1)}{\sum_{j=1}^{3} w_{ij}(x_1)}$$

with $1 \le j \le M$

Table 2: Comparative table of the criterion J_i

M	J_6	J_5	J_4	J_3 J_2	J_1	
4	1:12 10^{-6}	1:39 10^{-5}	1:6 10^{-6}	2:2 10^{-4}	8:47 10^{-7}	2:7 10^{-3}
3	1:24 10^{-5}	1:94 10^{-5}	6:86 10^{-6}	2:4 10^{-4}	1:3 10^{-5}	0.012
2	1 10^{-4}	4:4 10^{-4}	2:78 10^{-5}	3:2 10−3	1:5 10^{-4}	0.035
M	**J_7**	**J_8**	**J_9**	**J_{10} J_{11}**	**J_{12}**	
4	7:4 10^{-5}	4:8 10^{-6}	4:5 10^{-6}	1:6 10^{-6}	4:3 10^{-6}	2:2 10^{-6}
3	1 10^{-4}	1:8 10^{-5}	1:8 10^{-5}	2:9 10^{-6}	5:1 10^{-6}	7 10^{-6}
2	2:6 10^{-4}	1:6 10^{-4}	4:5 10^{-5}	1:2 10^{-5}	1:4 10^{-5}	7:1 10^{-6}

Table 3: Number of local models retained for each parameter function $\hat{K}_i(x_1)$

	K1	K2	K3	K4	K5	K6	K7	K8	K9	K10	K11	K12
M	3	3	3	2	3	3	3	2	2	2	2	2

Table 4: Parameters α_{ij} and β_{ij} of the local models

Fonction $\hat{K}_i(x_1)$	α_{i1}	α_{i2}	α_{i3}	β_{i1}	β_{i2}	β_{i3}
$\hat{K}_1(x_1)$	-0.04047	-0.00037	0.11230	5.0588	1.2314	-5.8506
$\hat{K}_2(x_1)$	-0.00003	0.00027	0.00134	0.07519	0.0424	0.00031
$\hat{K}_3(x_1)$	0.02394	-0.02435	0.028317	-3.04046	1.13799	-0.6829
$\hat{K}_4(x_1)$	0.00047	0.00085	-	-0.0234	0.04117	-
$\hat{K}_5(x_1)$	-0.00404	-0.00123	0.00234	0.4189	0.1777	-0.02158
$\hat{K}_6(x_1)$	-0.000049	-0.000002	0.000037	0.00590	0.00324	0.00122
$\hat{K}_7(x_1)$	-0.4575	0.66200	-1.5222	16.5531	-14.6319	13.8271
$\hat{K}_8(x_1)$	-0.05779	-0.0843	-	4.0511	12.5300	-
$\hat{K}_9(x_1)$	8.1252	4.8809	-	855.90	-17.841	-
$\hat{K}_{10}(x_1)$	0.6718	0.6578	-	34.157	31.048	-
$\hat{K}_{11}(x_1)$	-0.0474	0.0777	-	24.222	-0.0945	-
$\hat{K}_{12}(x_1)$	8.766	8.2391	-	370.93	124.52	-

For each parameter function, Table 1 provides only eight different values. If we try to represent a parameter function described by M = 3 local models, the dimension of the unknown parameter vector is equal to 12 (α_{ij}, β_{ij}, a_{ij}, b_{ij}, j = 1, ..., 3, for each i). Therefore, the estimation of these parameters cannot be achieved.

In fact, when implementing the model described by (1-2) and Table 1, the practitioner uses a linear interpolation of data given by the look-up table. As the purpose of this study essentially concerns the substitution of the lookup model by an analytical one, we have artificially generate, using a linear interpolation between the data of Table 1, a new table comprising N = 50 linearly equally spaced values between $x_{1,min}$ = 33:58 et $x_{1,max}$ = 93:48. The parameter estimation was done on the basis of this augmented table. A very classical least-squares method was implemented. For each parameter function, the used quadratic criterion is defined as follows:

$$J_i(\theta_i) = \frac{1}{2}\sum_{t=1}^{N} \varepsilon(t, \theta_i)^2 = \sum_{t=1}^{N}\left(K_i(x_1) - \hat{K}(x_1)\right)^2 \quad (6)$$

where J_i is the criterion to be minimized with regard to the ith parameter vector $\theta_i = [\alpha_{i1}, ..., \alpha_{1M}, \beta_{i1}, ..., \beta_{1M}, a_{i1}, ..., a_{1M}, b_{i1}, ..., b_{1M}]$.

For each parameter function, the parameter estimation was done using d ifferent number of local models. Table 2 shows the obtained residual criteria for M = {2, 3, 4}. Clearly this residual criteria are decreasing functions of the number M of local models. However, this table helps to do the compromise between the complexity of the chosen model and its accuracy.

Table 3 points out the number M of local models kept for every function $\hat{K}_i(x_1)$ for i = {1, 12}.

The parameters α_{ij} and β_{ij} of the local models obtained after optimization are presented in the Table 4. The parameters of the activation functions are shown in Table 5 in the case of three local models (M = 3) and in Table 6 in the case of only two local models (M = 2).

The results of identification are shown in Fig. 2. We notice that the multiple models $\hat{K}_i(x_1)$ give good approximation of the gains given in Table 1.

Nonlinear model simulation: By replacing the gains defined in the Table 1 by their corresponding multiple models $\hat{K}_i(x_1)$, we obtain a nonlinear model of the turbojet engine:

Table 5: Parameters of the activation functions

	$\mu_{11}(x_1)$	$\mu_{12}(x_1)$	$\mu_{13}(x_1)$	$\mu_{21}(x_1)$	$\mu_{22}(x_1)$	$\mu_{23}(x_1)$	$\mu_{31}(x_1)$	$\mu_{32}(x_1)$	$\mu_{33}(x_1)$
a_{ij}	-74.48	1.127	-0.312	4.120	0.110	-0.196	3.985	0.194	-0.691
b_{ij}	38.651	80.254	58.656	75.673	96.139	36.225	73.016	88.548	43.464

	$\mu_{51}(x_1)$	$\mu_{52}(x_1)$	$\mu_{53}(x_1)$	$\mu_{61}(x_1)$	$\mu_{62}(x_1)$	$\mu_{63}(x_1)$	$\mu_{71}(x_1)$	$\mu_{72}(x_1)$	$\mu_{73}(x_1)$
a_{ij}	5.110	0.519	-0.312	7.509	0.7488	-0.254	78.256	-0.158	-0.016
b_{ij}	66.809	88.263	65.211	61.458	84.892	68.096	67.810	97.594	26.043

Table 6: Parameters of the activation functions

	$\mu_{41}(x_1)$	$\mu_{81}(x_1)$	$\mu_{91}(x_1)$	$\mu_{101}(x_1)$	$\mu_{111}(x_1)$	$\mu_{121}(x_1)$
a_{ij}	110.3	38.46	113.06	46.97	123.35	21.87
b_{ij}	47.89	63.46	22.94	11.66	25.34	20.94

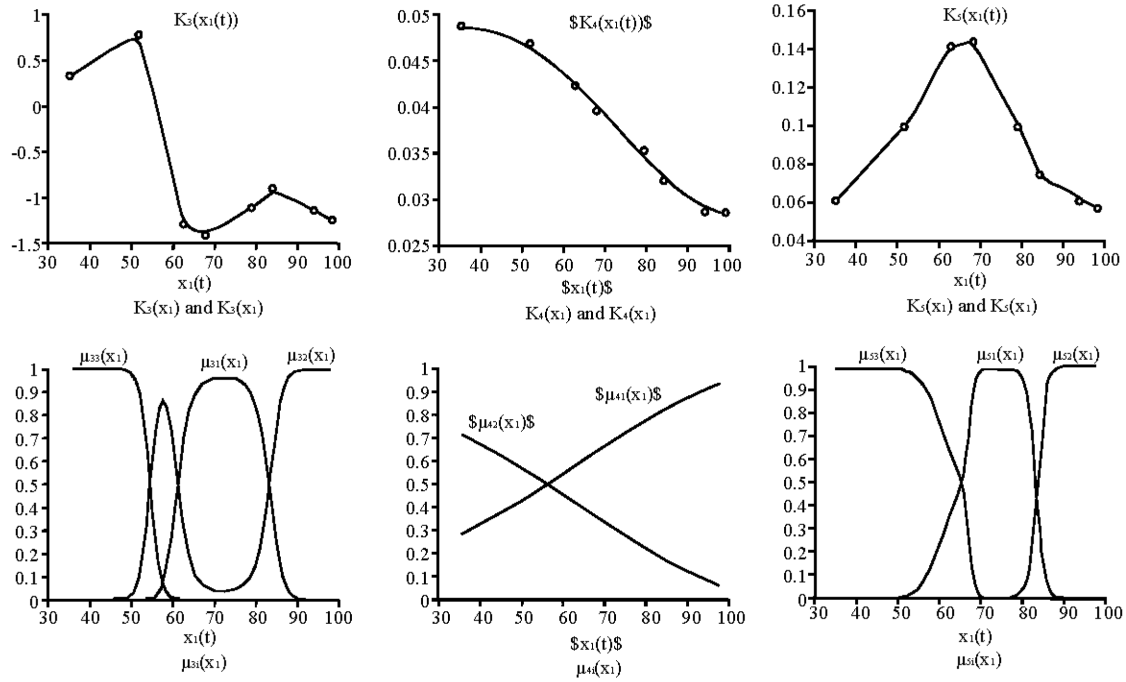

Fig. 2: Parameter functions and their activation's functions

$$\begin{cases} \dot{x}_1 = \hat{K}_1(x_1)\left(x_2 - \hat{K}_{10}(x_1)\right) + \hat{K}_2(x_1)\left(u - \hat{K}_9(x_1)\right) \\ \dot{x}_2 = \hat{K}_3(x_1)\left(x_2 - \hat{K}_{10}(x_1)\right) + \hat{K}_4(x_1)\left(u - \hat{K}_9(x_1)\right) \end{cases} \quad (7)$$

$$\begin{cases} y_1 = x_1 \\ y_2 = x_2 \\ y_3 = \hat{K}_5(x_1)\left(x_2 - \hat{K}_{10}(x_1)\right) + \hat{K}_6(x_1)\left(u - \hat{K}_9(x_1)\right) + \hat{K}_{11}(x_1) \\ y_4 = \hat{K}_7(x_1)\left(x_2 - \hat{K}_{10}(x_1)\right) + \hat{K}_8(x_1)\left(u - \hat{K}_9(x_1)\right) + \hat{K}_{12}(x_1) \end{cases} \quad (8)$$

In order to simplify the notation, the state and the output of the model (7-8) are already denoted by x and y even if they are different from the original state and output of model (1-2).

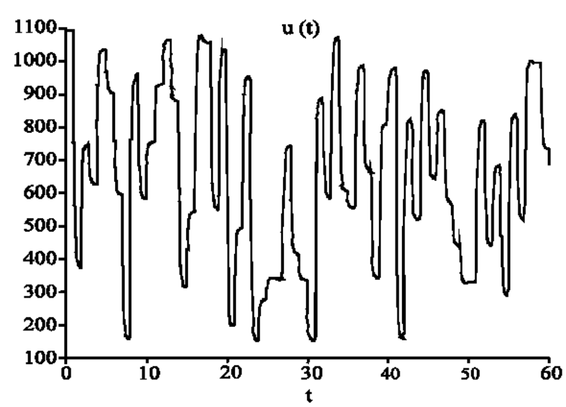

Fig. 3: Input u

The Fig. 3 shows the evolution of the input u, the Fig. 4 shows the comparison between the output vector

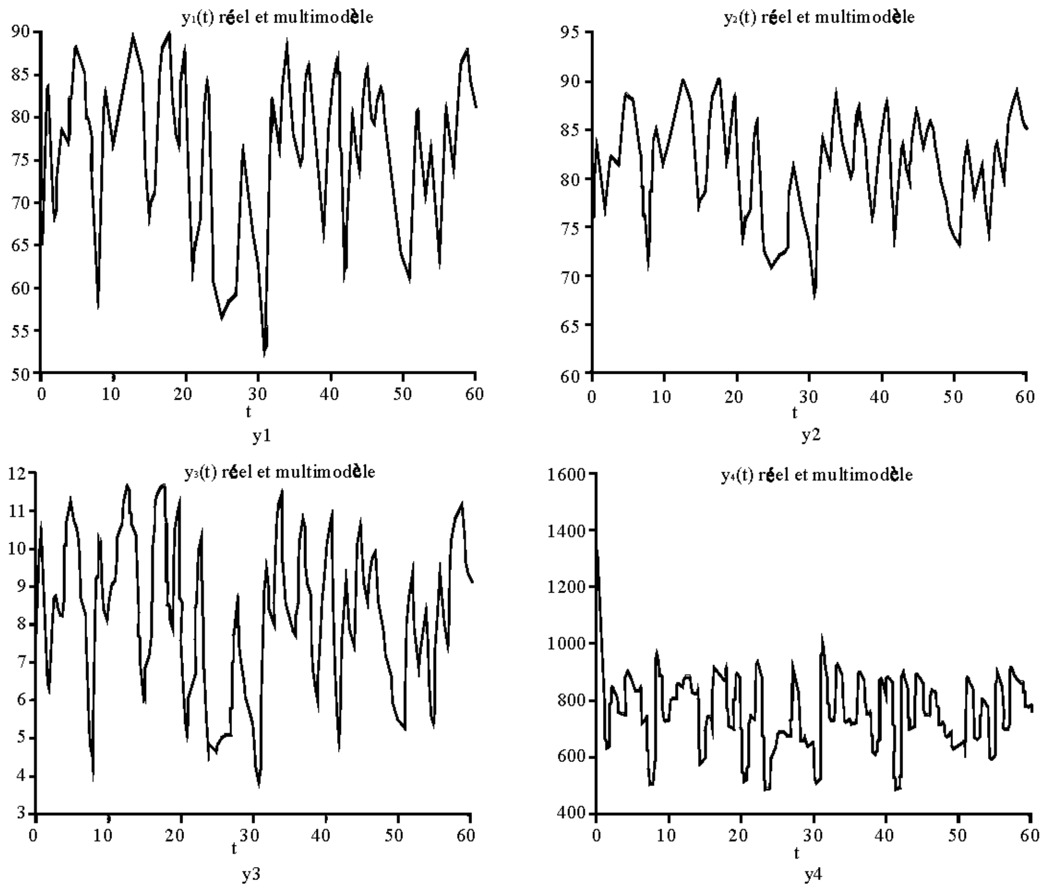

Fig. 4: Approximation of the look-up model by a nonlinear model

of the lookup model (1) and (2) and its approximate from the nonlinear model (7), (8) (these outputs match perfectly).

In conclusion, the proposed analytic nonlinear model allows the replacement of the table with a continuous model; so, during the simulation of the model any mechanism of interpolation in tables is needless. The synthesis of observer or controller for a nonlinear model is often delicate, then to have an exploitable model of the turbojet engine, we preferred to represent this turbojet by a multiple model.

Representation of the turbojet engine by a multiple model: The second step of the proposed modelling approach is to transform the analytical nonlinear model obtained previously in a multiple model form. This transformation is obtained by the mean of linearization technique of the nonlinear model (7) and (8) around operating points (Abonyi *et al.*, 2001; Teixeira and Stanislow, 1999). The i^{th} local model is obtained by linearizing the nonlinear model around operating point x_{1i}, x_{2i}, u_i. The activation functions v_i are only related to the input u and are chosen of triangular form. As the several analytical description of these activation functions is tiresome, the Fig. 5 illustrates their structure in the case of four local models. The values ui correspond to the considered operating points.

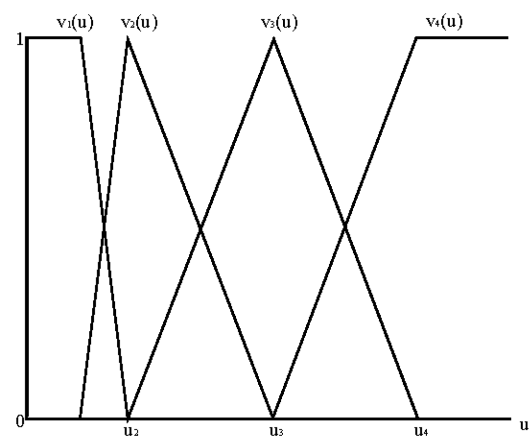

Fig. 5: Active functions v_i (u), i = {1, ..., 4}

Table 7: Comparative table of the criterion J

M	2	3	4
J	3.257	0.810	0.688

Table 8: The three operating points

i	x_{1i}	x_{2i}	u_i
1	65.88	66.87	344.25
2	72.37	80.43	557.01
3	90.07	85.05	1033.71

Then, the state equations of the multiple model are:

$$\begin{cases} \dot{x}_{m1} = \sum_{i=1}^{M} \nu_i(u)(A_{11i}x_{m1} + A_{12i}x_{m2} + B_{1i}u + D_{1i}) \\ \dot{x}_{m2} = \sum_{i=1}^{M} \nu_i(u)(A_{12i}x_{m1} + A_{22i}x_{m2} + B_{2i}u + D_{2i}) \end{cases} \quad (9)$$

The structure of the output equations is copied from that of the original model (1) and (2):

$$\begin{cases} y_{m1} = x_{m1} \\ y_{m2} = x_{m2} \\ y_{m3} = \sum_{i=1}^{M} \nu_i(u)(C_{11i}x_{m1} + C_{12i}x_{m2} + E_{1i}u + N_{1i}) \\ y_{m4} = \sum_{i=1}^{M} \nu_i(u)(C_{21i}x_{m1} + C_{22i}x_{m2} + E_{2i}u + N_{2i}) \end{cases} \quad (10)$$

The resulting matrices are (j = {1, 2} and i = {1, ..., M}):

$$A_{1ji} = \frac{\partial}{\partial x_j}\left[\hat{K}_1(x_1)\left(x_2 - \hat{K}_{10}(x_1)\right) + \hat{K}_2(x_1)\left(u - \hat{K}_9(x_1)\right)\right]\Bigg|_{\substack{x_1 = x_{1i} \\ x_2 = x_{2i} \\ u = u_i}}$$

$$A_{2ji} = \frac{\partial}{\partial x_j}\left[\hat{K}_3(x_1)\left(x_2 - \hat{K}_{10}(x_1)\right) + \hat{K}_4(x_1)\left(u - \hat{K}_9(x_1)\right)\right]\Bigg|_{\substack{x_1 = x_{1i} \\ x_2 = x_{2i} \\ u = u_i}}$$

$$B_{1i} = \frac{\partial}{\partial u}\left[\hat{K}_1(x_1)\left(x_2 - \hat{K}_{10}(x_1)\right) + \hat{K}_2(x_1)\left(u - \hat{K}_9(x_1)\right)\right]\Bigg|_{\substack{x_1 = x_{1i} \\ x_2 = x_{2i} \\ u = u_i}}$$

$$B_{2i} = \frac{\partial}{\partial u}\left[\hat{K}_3(x_1)\left(x_2 - \hat{K}_{10}(x_1)\right) + \hat{K}_4(x_1)\left(u - \hat{K}_9(x_1)\right)\right]\Bigg|_{\substack{x_1 = x_{1i} \\ x_2 = x_{2i} \\ u = u_i}}$$

$$C_{1ji} = \frac{\partial}{\partial x_j}\left[\hat{K}_5(x_1)\left(x_2 - \hat{K}_{10}(x_1)\right) + \hat{K}_6(x_1)\left(u - \hat{K}_9(x_1)\right) + \hat{K}_{11}(x_1)\right]\Bigg|_{\substack{x_1 = x_{1i} \\ x_2 = x_{2i} \\ u = u_i}}$$

$$C_{21ji} = \frac{\partial}{\partial x_j}\left[\hat{K}_7(x_1)\left(x_2 - \hat{K}_{10}(x_1)\right) + \hat{K}_8(x_1)\left(u - \hat{K}_9(x_1)\right) + \hat{K}_{12}(x_1)\right]\Bigg|_{\substack{x_1 = x_{1i} \\ x_2 = x_{2i} \\ u = u_i}}$$

$$E_{1ji} = \frac{\partial}{\partial u}\left[\hat{K}_5(x_1)\left(x_2 - \hat{K}_{10}(x_1)\right) + \hat{K}_6(x_1)\left(u - \hat{K}_9(x_1)\right) + \hat{K}_{11}(x_1)\right]\Bigg|_{\substack{x_1 = x_{1i} \\ x_2 = x_{2i} \\ u = u_i}}$$

$$E_{2ji} = \frac{\partial}{\partial u}\left[\hat{K}_7(x_1)\left(x_2 - \hat{K}_{10}(x_1)\right) + \hat{K}_8(x_1)\left(u - \hat{K}_9(x_1)\right) + \hat{K}_{12}(x_1)\right]\Bigg|_{\substack{x_1 = x_{1i} \\ x_2 = x_{2i} \\ u = u_i}}$$

$$\begin{aligned} D_{1i} &= \hat{K}_1(x_{1i})(x_{2i} - \hat{K}_{10}(x_{1i})) + \hat{K}_2(x_{1i}) \\ &\quad (u_i - \hat{K}_9(x_{1i})) - A_{12i}x_{2i} - B_{1i}u_i \\ D_{2i} &= \hat{K}_3(x_{1i})(x_{2i} - \hat{K}_{10}(x_{1i})) + \hat{K}_4(x_{1i}) \\ &\quad (u_i - \hat{K}_9(x_{1i})) - A_{22i}x_{2i} - B_{2i}u_i \\ N_{1i} &= \hat{K}_5(x_{1i})(x_2 - \hat{K}_{10}(x_{1i})) + \hat{K}_6(x_{1i})(u_i - \hat{K}_9(x_{1i})) \\ &\quad + \hat{K}_{11}(x_{1i})) - C_{11i}x_{1i} - C_{12i}x_{2i} - E_{1i}u_i \\ N_{2i} &= \hat{K}_7(x_{1i})(x_{2i} - \hat{K}_{10}(x_{1i})) + \hat{K}_8(x_{1i})(u_i - \hat{K}_9(x_{1i})) \\ &\quad + \hat{K}_{12}(x_{1i})) - C_{21i}x_{1i} - C_{22i}x_{2i} - E_{2i}u_i \end{aligned}$$

The number of local models was chosen by minimizing a quadratic criterion with respect parameter vector θ, function of the variation between values given by the model (7), (8) and those given by the multiple model (9) and (10). The used criterion is the following:

$$J(\theta)\sum_{t=0}^{t_f}\sum_{i=1}^{4}\left(\frac{y_i - y_{mi}}{y_{i\max} - y_{i\min}}\right)^2 \tag{11}$$

with t_f is the experiment length, $\theta = [x_{11}, x_{21}, u_1, ..., x_{1M}, x_{2M}, u_M]$, $y_{i\max}$ and $y_{i\min}$ represents respectively the maximal and minimal values of the vector y_i for $i \in \{1, 4\}$. The criterion $J(\theta)$ (11) is weighted because of the great disparity between the values of variables y_i.

The method which we adopted to determine the number of local models is the same as the one employed to approximate gains. We made various simulations changing the number M of local models from 1 to 4. The values of different criteria are shown in Table 7.

We then chose M = 3 by performing a compromise between quality and complexity. The numerical values of the obtained operating points are given on the Table 8. The corresponding activation functions are depicted in Fig. 6.

The structure of the different matrices A_i, B_i, F_i, C_i, D_i and H_i is the following:

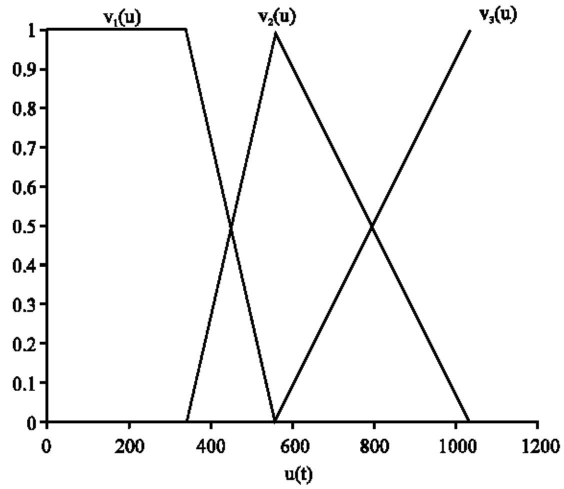

Fig. 6: Activation functions $v_i(u)$

$$A_i = \begin{pmatrix} A_{11i} & A_{12i} \\ A_{12i} & A_{22i} \end{pmatrix}, B_i = \begin{pmatrix} B_{1i} \\ B_{2i} \end{pmatrix}, D_i = \begin{pmatrix} D_{1i} \\ D_{2i} \end{pmatrix}$$

$$C_i = \begin{pmatrix} 1 & 0 \\ 0 & 1 \\ C_{11i} & C_{12i} \\ C_{12i} & C_{22i} \end{pmatrix}, E_i = \begin{pmatrix} 0 \\ 0 \\ E_{1i} \\ E_{2i} \end{pmatrix}, N_i = \begin{pmatrix} 0 \\ 0 \\ N_{1i} \\ N_{2i} \end{pmatrix}$$

and their numerical values are:

$$A_1 = \begin{bmatrix} -2.427 & 2.323 \\ 0.00223 & -1.424 \end{bmatrix}, A_2 = \begin{bmatrix} -2.652 & 2.0442 \\ -0.366 & -1.1970 \end{bmatrix}, A_3 = \begin{bmatrix} -3.107 & 1.295 \\ -0.350 & -0.935 \end{bmatrix}$$

$$B_1 = \begin{bmatrix} 0.072 \\ 0.040 \end{bmatrix}, B_2 = \begin{bmatrix} 0.073 \\ 0.036 \end{bmatrix}, B_3 = \begin{bmatrix} 0.065 \\ 0.031 \end{bmatrix}$$

$$D_1 = \begin{bmatrix} -46.146 \\ 89.543 \end{bmatrix}, D_2 = \begin{bmatrix} -7.165 \\ 102.366 \end{bmatrix}, D_3 = \begin{bmatrix} 93.974 \\ 85.076 \end{bmatrix}$$

$$C_1 = \begin{bmatrix} 1 & 0 \\ 0 & 1 \\ 0.054 & 0.145 \\ -2.185 & -9.680 \end{bmatrix}, C_2 = \begin{bmatrix} 1 & 0 \\ 0 & 1 \\ 0.108 & 0.1150 \\ -6.752 & -6.893 \end{bmatrix}, C_3 = \begin{bmatrix} 1 & 0 \\ 0 & 1 \\ 0.130 & 0.0678 \\ -6.729 & -2.670 \end{bmatrix}$$

$$E_1 = \begin{bmatrix} 0 \\ 0 \\ 0.003 \\ 0.772 \end{bmatrix}, E_2 = \begin{bmatrix} 0 \\ 0 \\ 0.003 \\ 0.586 \end{bmatrix}, E_3 = \begin{bmatrix} 0 \\ 0 \\ 0.003 \\ 0.441 \end{bmatrix}$$

$$N_1 = \begin{bmatrix} 0 \\ 0 \\ -9.8 \\ 1254.3 \end{bmatrix}, N_2 = \begin{bmatrix} 0 \\ 0 \\ -11.3 \\ 1471.6 \end{bmatrix}, E_3 = \begin{bmatrix} 0 \\ 0 \\ -9.5 \\ 1260.2 \end{bmatrix},$$

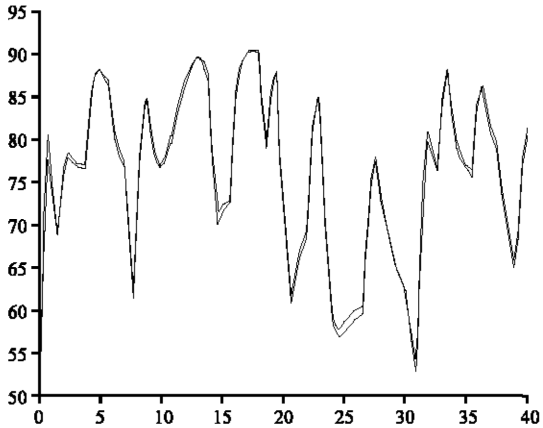

Fig. 7: Output $y_{m1}(t)$ of the multiple model and the nonlinear model

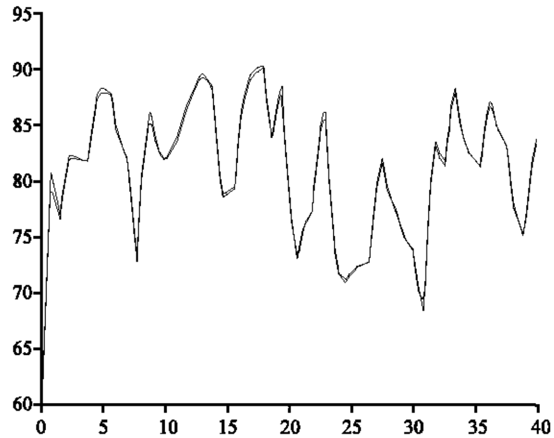

Fig. 8: Output $y_{m2}(t)$ of the multiple model and the nonlinear model

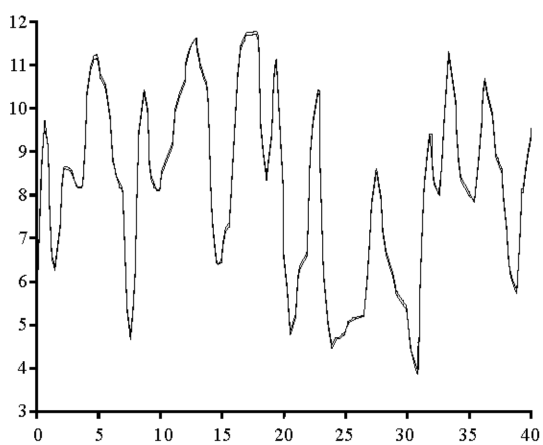

Fig. 9: Output $y_{m3}(t)$ of the multiple model and the nonlinear model

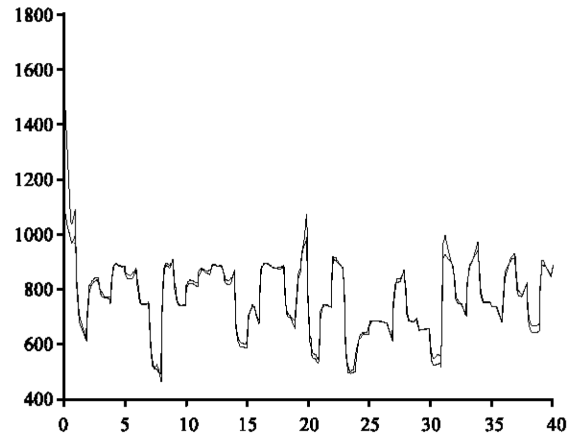

Fig. 10: Output $y_{m4}(t)$ of the multiple model and the nonlinear model

Thus, the model obtained is easier to exploit than the initial model described by the Table 1. It can be of a particular utility for designing diagnosis method for the turbojet based on classical techniques (development of a multiple observer).

Simulation of the model of the turbojet: In order to check the good accuracy of the multiple model, we simulate two models in parallel: the multiple model 9, 10 and the nonlinear model 7, 8. The applied input is the same as the one used to identify the parameters of the gains Ki(x1).

Figure 7-10 show the superposition of the output vector of the nonlinear model 7 and 8 of the turbojet and their approximation by the multiple model 9 and 10.

CONCLUSION

In this study, we showed how to build, from a nonlinear look-up model of a physical system (turbojet engine), a multiple model based on several linear local models. The results of simulation show the capacity of the multiple models to approximate the behavior of the nonlinear system.

The increase of the number of local models allows to take into account the complexity of the system and also allows to reach the desired precision of the global model according to aims in view's.

The proposed modelling was carried out in two stages: the parameter functions $K_i(x_1)$ are First termed into multiple model in order to obtain an analytical nonlinear model and next the nonlinear model is linearized to obtain the Final multiple model.

However, it is possible to obtain the same results in one step. In this case, the multiple model would have been directly given starting from the experimental data after, having a structure being imposed. The principal disadvantage of this last approach lies in the number of parameters to identify which is larger than the number of operating points chosen previously.

REFERENCES

Abonyi, J., R. Babuska and F. Szeifert, 2001. Fuzzy modeling with multivariate membership functions: Gray-box identification and control design. IEEE. Trans. Sys. Man Cybernetics, 31: 755-767.

Gasso, K., G. Mourot and J. Ragot, 2000. Identification of an output error takagi-sugeno model. IEEE. International Conference on Systems. Man and Cybernetics, 1: 14-19.

Harefors, M., 1997. Application of h robust control to the rm12 jet engine. Control Eng. Pract., 5: 1189-1201.

Johansen, T.A. and A.B. Foss, 1993. Constructing narmax using armax. Int. J. Control, 58: 1125-1153.

Mueller, G.S., 1971. Linear model of a 2-shaft turbojet and its properties. Inst. Electric. Eng., pp: 813-815.

Murray-Smith, R., 1997. Multiple model approaches to modelling and control. Taylor and Francis.

Savy, A., 2003. Diagnostic de défauts capteurs sur turboréacteur. Ph.D Thesis, Institut National Polytechnique de Lorraine, Vandoeuvre-l es-Nancy, France.

Silva, D., 1982. Real time failure detection of aircraft engine output sensor. Arab. J. Sci. Eng., 7: 45-53.

Tanaka, K., T. Ikeda and H.O. Wang, 1996. Robust stabilisation of a class of uncertain nonlinear system via fuzzy control: Quadratic stability, H 1 control theory and LMIs. IEEE. Trans. Fuzzy Sys., 4: 1-12.

Teixeira, C.M. and H. Stanislaw, 1999. Stabilising controller design for uncertain nonlinear systems using fuzzy models. IEEE. Trans. Fuzzy Sys., 7: 133-142.

Trevino, L.C. and S. Olcmen, 2003. Use of soft computing technologies for rocket engine control. IEEE. Digital Avionics Sys. Conf., 1: 3A11-3A17.

Wang, H.O., K. Tanaka and M. Griffin, 1996. An approach to fuzy control of nonlinear system: Stability and design issues. IEEE. Trans. Fuzzy Sys., 4: 14-23.

Wells and D. Silva, 1977. Failure diagnosis for in bilinear systems-a survey. Automatic Control Conf., pp: 1493-149.

Wu, X. and G. Campion, 2004. Fault detection and isolation of systems with slowly varying parameters simulation with a simplified aircraft turbo engine model. Mech. Sys. Signal Proces., 18: 353-366.